Repeatability and reproducibility of oxygen-enhanced MRI of the lung at 3 tesla: cross-center, cross-vendor evaluation

Mina Kim¹, Sarah H. Needleman¹, Josephine H. Naish^{2,3}, Yohn Taylor¹, Marta Tibiletti², James P. B. O'Connor^{4,5}, and Geoff J. M. Parker^{1,2}

¹Centre for Medical Image Computing (CMIC), Department of Medical Physics & Biomedical Engineering, University College London, London, United Kingdom, ²Bioxydyn Limited, Manchester, United Kingdom, ³BHF Manchester Centre for Heart and Lung Magnetic Resonance Research (MCMR), Manchester, United Kingdom, ⁴Division of Cancer Sciences, University of Manchester, Manchester, United Kingdom, ⁵Division of Radiotherapy and Imaging, Institute of Cancer Research, Manchester, United Kingdom

Synopsis

A recently developed protocol with a dual echo RF-spoiled gradient echo acquisition enabled simultaneous measurement of dynamic OE signal change and the substantial ΔR_2^* effect at 3 tesla. To progress towards clinical translation, we evaluated repeatability and reproducibility across two sites, vendors and time points. Our results demonstrate good repeatability for the quantitative and semi-quantitative indices across time points, consistent signal behaviour and repeatable ΔR_2^* across two sites and vendors, suggesting potential utility in multi-centre clinical studies. However, echo time dependence should be considered when interpreting percentage signal enhancement.

Introduction

Oxygen-enhanced MRI (OE-MRI) can provide information on regional lung function [1]. Despite technical challenges of OE-MRI in the lung at higher magnetic field, we have recently shown the feasibility of lung OE-MRI at 3 T and signal enhancement behaviour in the lung using a dual echo RF-spoiled gradient echo acquisition [2]. This method enables measurement of dynamic OE signal change with either T_1 -weighting or T_2 *-weighting, and for monitoring of dynamic ΔR_2 * [2,3]. To translate these biomarkers into clinical use, they must demonstrate their repeatable and reproducible assessment of lung function. The purpose of this work was to evaluate the proposed method across two sites, vendors and time points.

Subjects & Methods

Following research ethics approval and written informed consent, we recruited 16 healthy volunteers with no previous record of lung diseases. Of these, 8 travelling subjects (3 males, age range = 26-54 years, median = 39.5) underwent lung MRI on a 3 T whole-body scanner from two vendors in different cities (Philips Ingenia in London, UK and Siemens MAGNETOM Vida in Manchester, UK) at a 4 week interval. Eight separate subjects (4 males, age range = 23-51 years, median = 27) were scanned twice for a scan-rescan test at a 4-6 week interval using the Philips scanner. Scan parameters for the RF-spoiled dual gradient echo acquisition for each vendor are listed in Table 1. Selection of flip angle (FA) was optimized through simulation (Fig. 1) by varying FA and TE values [2,4]. The shortest TE values available for the chosen acquisition were selected for each scanner: $TE_{1A} = 0.71$ ms, $TE_{2A} = 1.2$ ms for Philips; $TE_{1B} = 0.71$ 0.81 ms, $TE_{2B} = 1.51$ ms for Siemens. Subjects breathed medical air (21% O_2) and 100% O_2 via non-rebreathing face mask (Intersurgical Ltd., Wokingham, UK) at a flow rate of 15 Lmin⁻¹. Images were acquired during free breathing. Data analysis was performed in MATLAB R2022b (MathWorks, Natick, MA). After non-linear image registration using ANTs [5,6], the lung parenchyma, excluding central major vasculature, was manually segmented from registered images and a voxel-wise tissue density correction was applied. Subsequently, the dynamic data points in the masked lung were fitted using exponential functions for the O₂ wash-in and wash-out with least-squares algorithm for each voxel. Percent signal enhancement (PSE) maps were produced by the subtraction of the fitted baseline normoxia intensity from the fitted hyperoxia intensity, normalized to the fitted normoxia intensity. Mean and standard deviation (std) were calculated for PSE values at each TE over 6 slices for TE_{1A}, TE_{1B}, TE_{2A} and 2 most posterior slices only for TE_{2B} due to poor signal to noise ratio (SNR) in the anterior slices at TE_{2B} . Mean ΔR_2 * maps were calculated by the subtraction of averaged normoxia R_2 * maps (30th to 60th time series acquisitions) from averaged hyperoxia R_2 * maps (120th to 180th). Intra-class correlation coefficient (ICC) was calculated using SPSS v28.0 (SPSS Inc, Chicago, IL).

Results

Simulations show that T_2 *-induced negative enhancement (Δ S) is maximum at FA ~5° independent of the choice of TE (Fig. 1A), and TE dependence of Δ S reduces with smaller FA (Fig. 1B). Negative PSE increases with lower FA and longer TE (Fig. 1C).

Representative volunteer PSE maps at TE_{1A} (Fig 2A), TE_{2A} (Fig. 2B) and $\triangle R_2^*$ (Fig. 2C) demonstrate good intra-scanner, intra-subject repeatability, confirmed by Bland-Altman analysis (Fig. 2D-F) (Philips in London). PSE maps from interscanner, intra-subject repeat scans show similar spatial distribution of the enhancement signal at TE₁ while the signal at TE₂ from the Manchester site is compromised due to low SNR caused by longer TE (Fig. 3A). Plots of the combined PSE values at 4 separate TEs from two MRI systems display TE dependence of the signal (Fig. 3B, Table 2) similar to simulation expectations. The inter-scanner variability (\pm std of the parameter differences between two scanners when the same volunteer was scanned) and the intra-scanner variability (between two sessions when the same volunteer was scanned) show good repeatability and reproducibility of the indices (Table 2), confirmed by $\triangle R_2^*$ maps and Bland-Altman analysis (Fig. 3C, 3D). High ICC values are observed for both inter-scanner and intra-scanner $\triangle R_2^*$ comparisons (Table 2).

Discussion

Our results show that the proposed protocol with a dual echo RF-spoiled gradient echo acquisition at 3 T yields excellent intra-scanner repeatability. They also demonstrate that comparable OE-MRI protocols of the lung can be implemented at 3 T across different sites and scanners with good repeatability and reproducibility for $\triangle R_2^*$. Although matching TE between scanners is challenging, the expected trend of PSE with TE is observed between sites.

Conclusions

We have evaluated repeatability and reproducibility of OE-MRI of the lung at 3 T across two sites, vendors and time points using a dual echo RF-spoiled gradient echo acquisition. Our results demonstrate good repeatability for the quantitative and semi-quantitative indices across time points, consistent signal behaviour and repeatable ΔR_2 * across two sites and vendors, suggesting potential utility in multi-centre clinical studies. However, substantial impact of TE should be considered when interpretating PSE.

Acknowledgements

This work is supported by the Cancer Research UK National Cancer Imaging Translational Accelerator (NCITA) awards C1519/A28682 (UCL) and C19221/A28683 (University of Manchester), the EPSRC-funded UCL Centre for Doctoral Training in Medical Imaging (EP/L016478/1; EP/S021930/1), an EPSRC Industrial CASE award (Voucher No. V20000074), GlaxoSmithKline Research and Development Ltd (BIDS3000035683), and Innovate UK award 104629. We thank Lucy Caselton, Sumandeep Kaur and David M. Higgins for the technical assistance.

References

- 1. Edelman RR et al., Noninvasive assessment of regional ventilation in the human lung using oxygen-enhanced magnetic resonance imaging. Nat Med. 1996; 2: 1236–1239.
- 2. Kim M et al., Oxygen-enhanced MRI of the lung at 3 tesla: R₂* contrast in smokers and non-smokers. Proc Intl Soc Magn Reson Med. 2022; 1481.
- 3. S. H. Needleman et al., Functional Lung MRI at 3.0 T using Oxygen-Enhanced MRI (OE-MRI) and Independent Component Analysis (ICA), Proc Intl Soc Magn Reson Med. 2022; 658.
- 4. Kruger SJ et al. Oxygen-enhanced 3D radial ultrashort echo time magnetic resonance imaging in the healthy human lung. NMR Biomed. 2014; Dec;27(12):1535-41.
- 5. Avants BB et al. Symmetric diffeomorphic image registration with cross-correlation: evaluating automated labeling
- of elderly and neurodegenerative brain. Med Image Anal. 2008;12(1):26-41.

 6. Avants BB et al. A reproducible evaluation of ANTs similarity metric performance in brain image registration.
- Neurolmage. 2011;54(3):2033-2044.

 7. District at al. Outroop subspaced MDI of the lung at 3 Tables Facelbility and T. relevation times. Due of the lung at 3 Tables Facelbility and T. relevation times. Due of the lung at 3 Tables Facelbility and T. relevation times.

7. Dietrich et al. Oxygen-enhanced MRI of the lung at 3 Tesla: Feasibility and T_1 relaxation times. Proc Intl Soc Magn Reson Med. 2006; 14: 1307.

Figures

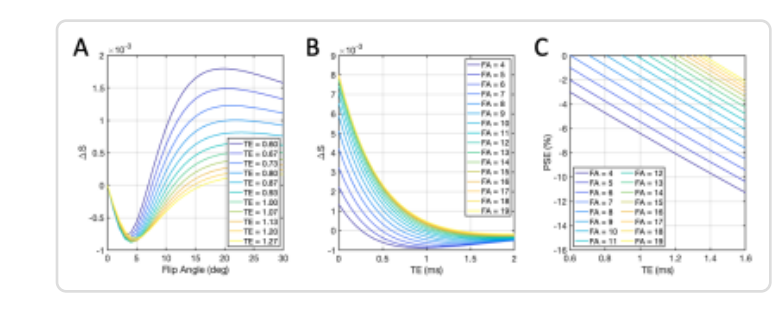


Figure 1. The expected OE signal enhancement (ΔS) for a dual echo spoiled gradient echo acquisition at 3 T due to ΔT_1 and ΔT_2* as a function of FA and TE (A and B), assuming literature-reported values for T₁ [7] and measured T₂* in the lungs at 21% and 100% oxygen (TR = 16 ms; T₁ (21% O₂) = 1281 ms, T₁ (100% O₂) = 1102 ms. T₂* (21% O₂) = 0.64 ms and T₂* (100% O₂) = 0.60 ms). (C) Corresponding percentage signal enhancement (PSE) as a function of TE using the same parameters as in Fig. 1A and 1B.

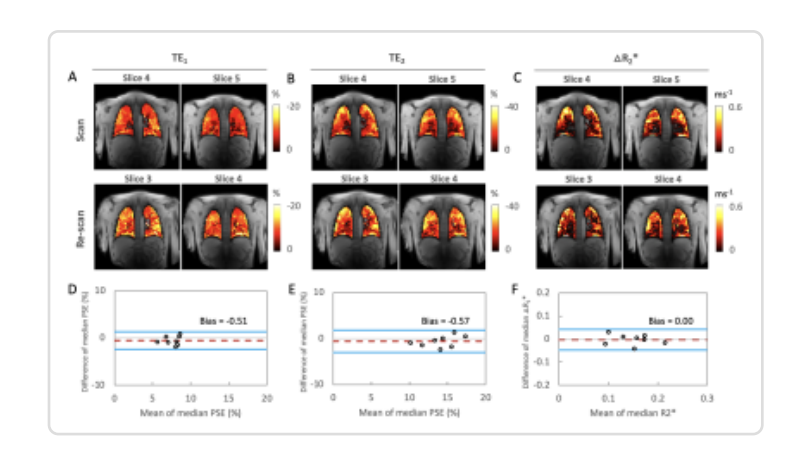


Figure 2. Representative intra-scanner, intra-subject repeatability (in London) of PSE at (A) TE_{1A} , (B) TE_{2A} and (C) $\triangle R_2$ *. Bland-Altman analysis comparing PSE and $\triangle R_2$ * between two separate sessions. (D) whole lung median PSE with $TE_{1A} = 0.71$ ms, (E) whole lung median PSE with $TE_{2A} = 1.2$ ms and (F) whole lung median $\triangle R_2$ *. The dashed red line indicates the bias, and the solid blue lines indicate the limits of agreement.

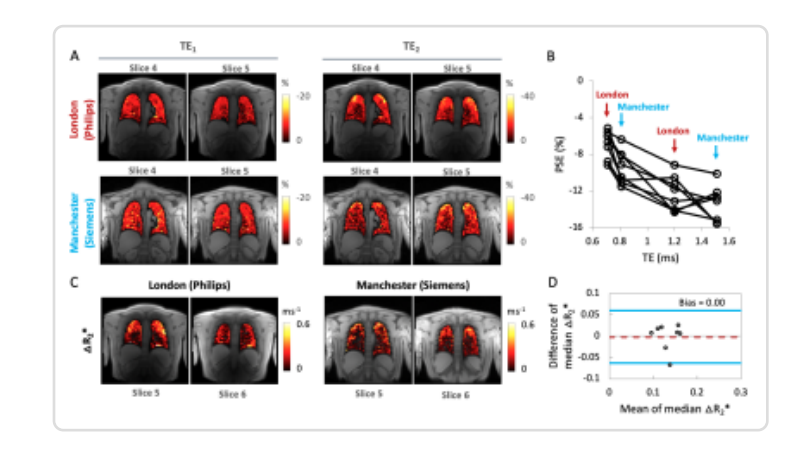


Figure 3. Representative inter-scanner intra-subject reproducibility of PSE at (A) TE₁ and TE₂ scanned using two MRI systems at two sites (London and Manchester). (B) PSE obtained at 4 separate echo times ($TE_{1A} = 0.71$ ms, $TE_{2A} = 1.2$ ms in London and $TE_{1B} = 0.81$ ms, $TE_{2B} = 1.51$ ms in Manchester). The combined PSE values from two MRI systems show the similar trend as a function of TE from simulation (Fig. 1C). (C) Inter-scanner intra-subject reproducibility of $\triangle R_2^*$ from the same subject. (D) Bland-Altman analysis comparing $\triangle R_2^*$ between two scanners for the same subjects.

	Scanner A (London)	Scanner B (Manchester)	
Manufacturer	Philips	Siemens	
Model	Ingenia	MAGNETOM Vida	
Field strength (T)	3.0	3	
RF coil used	32-channel torso coil in combination with the posterior coil	18 channel body coil combination with the 3 channel spine coil	
Max. gradient strength (mT/m)	45	45	
Max. slew rate (T/m/s)	200	200	
TR (ms)	16	16	
Echoes	full	half	
TE ₁ (ms)	0.71	0.81	
TE ₂ (ms)	1.2	1.51	
FOV (mm x mm)	450 x 450	450 x 450	
No of slices	6	6	
Slice thickness (mm)	10	10	
Gap (mm)	4	4	
Acquired matrix	96 x 96	96 x 96	
Orientation	Coronal	Coronal	
Pixel size (mm x mm)	4.7 x 4.7	4.7 x 4.7	
Flip Angle (degrees)	5	5	
Bandwidth (Hz/Px)	4488	2000	
Parallel Imaging	N	N	
NSA	1	1	
Time resolution (s)	1.54	1.54	
Number of dynamics	340	340	

Table 1. Scan parameters

	Mean ± std	Inter-scanner (intra-volunteer)	Intra-scanner (intra-volunteer)	ICC _{inter}	ICC _{intra}
TE _{1A} PSE	-6.81 ± 1.47	-	± 0.52		0.77
TE ₁₈ PSE	-9.46 ± 1.82	-	± 0.75	-	0.92
TE _{2A} PSE	-12.31 ± 1.90	-	-	-	-
TE ₂₈ PSE	-13.37 ± 1.91	-	-		-
ΔR ₂ *	0.14 ± 0.03	± 0.02	± 0.01	0.70	0.94

Table 2. Reproducibility and repeatability for PSE and $\triangle R_2^*$. The 1st column: the mean \pm std over all volunteers. The 2nd and 3rd column: the inter-scanner and the intra-scanner variability for the same volunteers scanned twice. The last two columns: intra-class correlation coefficient (ICC) for ICC_{inter} (ICC for interscanner) and ICC_{intra} (ICC for intra-scanner) based on absolute agreement, 2-way mixed-effects model.